Numerical Investigation of Saturated-Unsaturated Flow and Stability Analysis of Tailings Dams Considering the Influence of Saline Solutions

Mona Anbarestani[1], *Hamed Sadeghi*[1*], and *Ali Golaghaei Darzi*[1]

[1] Department of Civil Engineering, Sharif University of Technology, Tehran, Iran

Abstract. A tailings dam is normally constructed through self-consolidation with minimum compaction effort. Accordingly, special attention to the ultimate limit design in assessing the tailings dam instability condition is of primary importance. Furthermore, the existence of pore fluid chemical contaminants with high concentrations makes soil hydraulic and shear resistance properties subject to considerable changes. Therefore, this study aims to investigate the stability of a tailing dam using saturated-unsaturated flow analysis under 0.2 and 0.6 M sodium chloride solutions and pure water as a benchmark. To make the analyses as realistic as possible, recently developed solute-dependent hydraulic conductivity and water retention models are embedded into the numerical software. The results show that the saline-based model has higher pore water pressure than the pure water model due to more rainfall penetration by increasing the pore fluid salt concentration. Furthermore, increasing salt solution concentration enhances the tailing dam's drainage condition, which leads to an increase in the dam's shear strength and, consequently, the factor of safety. Therefore, the stability of the tailings dam is improved by the combined impact of salt on both the flow and strength.

1 Introduction

Tailings are the waste result of mining processes. They consist of sand and silt with high concentrations of metals and chemical contaminants during the extraction of raw materials. Tailings are usually discharged as a slurry into storage areas, technically referred to as tailings dams [1]. Water-retention and raised embankments are the two basic types of tailing dams. Tailings dams are built and raised to increase the stored capacity, often without interrupting the mining activities [1– 3]. Most tailings dams were built several decades ago, and about 45% of them are raised embankments, the least stable type of dam. The failure rate of raised tailings dams is approximately tenfold of the retention dams [4]. Statistics on failures mainly consider the physical failures ignoring the environmental hazards, such as groundwater or surface water pollution from tailings impoundments, which are also international issues. It is estimated that hydraulic factors, such as seepage, cause 38% of tailings dam failures [5]. Therefore, seepage is one of the most critical factors that affect the stability of the tailings dam and the environment of the reservoir area [6, 7].

Relatively extensive studies have been carried out to determine seepage discharge and slope stability of tailings dams using various numerical and experimental methods [3]. However, most of them follow a postulation that the pore fluid permeating through the soil voids is distilled water, which is most definitely not the case when dissolved ions are abundant in the water, as they can affect both the flow regime and stability [8].

According to recent studies, natural soil strata near the Gulf of Oman contain high concentrations of solute in the pore fluids [9]. Additionally, numerical simulations based on rigorous laboratory characterization of unsaturated soil properties confirmed that salinity significantly contributes to the instability of railroad embankments. The main reason is that the considerable amount of sodium in the natural aeolian strata affects the water retention and unsaturated hydraulic conductivity of soils [8]. In addition, exposure to saline environments results in a significant microstructural change that is reflected in the evolution of macro porosity, which primarily regulates flow characteristics [10, 11]. Consequently, seepage and stability of tailings dams are expected to change because of the presence of soluble salinity species in environments such as slurry tailings [6]. Furthermore, previous research has shown that salinity affects the mechanical properties of materials, which may affect the slope stability [12].

On the other hand, rainfall is an essential climatic element that affects the serviceability and failure of hydraulic structures such as tailings dams [13]. In recent years, extreme events, such as heavy rainfall, have been identified as the trigger in 25% of global and 35% of European tailings dam failures, also rainstorms in semiarid to arid regions subjected to prolonged drought periods, have exacerbated the failure of natural and artificial earth fill slopes [14]. Such slopes are in unsaturated states, and the stability conditions are satisfied by additional suction stress unless an anticipated rainfall is heavy enough to vanish most of the inter-particle suction stress contacts [15].

The main purpose of this analysis was to examine the comparative impact of salt on hydraulic and strength characteristics and its influence on the analysis of flow and stability, which had not been extensively explored in previous research. Therefore, this study is investigating the effect of sodium chloride solution concentrations on the stability of a tailings dam under

* Corresponding author: hsadeghi@sharif.edu

three months of real rainfall infiltrations. To achieve this objective, recent solute-dependen hydraulic conductivity and water retention models are used to estimate water retention and hydraulic characteristics. Furthermore, the input strength parameters are modified based on existing models as a function of the molar concentration in the numerical simulations.

2 Materials and properties

2.1 Studied mining area

The Sarcheshmeh tailings dam is considered as the case study. This tailings dam is located 19 km northwest of the Sarcheshmeh Copper Complex factory and 32 km southwest of Rafsanjan city in Kerman province, Iran. The dam was constructed in two phases. In the first phase in 1979, the dam was built as an earth-fill dam with a clay core. Its height was 75 m, and its reservoir volume was 123 Mm^3. In order to maintain the operation of the Sarcheshmeh copper mine, the tailing dam was 40 m raised in two stages, as shown in Fig. 1 [12, 16].

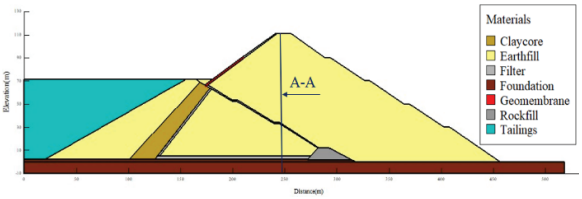

Fig. 1. The geometry of the Sarcheshmeh tailings dam.

2.2 Soil–water retention curve

The soil-water retention curve (SWRC) is one of the most important parameters for transient seepage analysis through an unsaturated soil. Accordingly, SWRCs for the materials are estimated using a recently developed model based on the van Genuchten model. The modified model can incorporate the effects of salt solution on soil fluid retention behavior as expressed in Eq. 1 [17, 18]:

$$\theta = \theta_r + (\theta_{salt} - \theta_r)\left\{1 + (\alpha_{sat}\psi)^n\right\}^{-m} \quad (1)$$

where ψ is the soil suction, θ is the volumetric water content, θ_{salt} is the saturated volumetric water content considering the effect of salt concentration, θ_r is the residual volumetric water content, α_{salt} is air entry value considering the effect of salt concentration, n, and m are fitting parameters. The values of these parameters for the earth fill and clay core sections of the dam under the effect of salt concentration materials are summarised in Table 1. The other parts of the dam are collected in Table 2.

Table 1. Input parameters of the SWRC and HCF models with various NaCl molar concentrations [19, 20].

Material	C (M)	θ_s	α_{salt}	k_s (m/s)
Earth fill	0	0.44	0.0455	5.63×10^{-8}
	0.2	0.39	0.0458	7.11×10^{-8}
	0.6	0.35	0.0461	7.43×10^{-8}
Clay core	0	0.53	0.0024	4.41×10^{-12}
	0.2	0.52	0.0026	9.12×10^{-12}
	0.6	0.51	0.0027	1.05×10^{-11}

Table 2. Input parameters of the SWRC and HCF models [21].

Material	θ_s	α	n	m	k_s (m/s)
Foundation	0.35	1.34	9.43	0.02	3.04×10^{-6}
Rock fill	0.38	0.13	7.38	0.19	2.28×10^{-5}
Filter	0.41	1.67	6.94	0.23	2.98×10^{-5}
Tailings	0.4	-	-	-	1.01×10^{-7}
Geomembrane	0.6	-	-	-	1×10^{-13}

Based on Eq. 1, the effects of salt concentration on the soil-water retention curve for clay core materials are depicted in Fig. 2. According to this figure, the retention capacity is reduced as molarity increases. Therefore, the SWRC inclines to the left, and the air entry suction decreases. When salt in the pore fluid enters the soil structure of clay materials, it decreases the thickness of the diffuse double layer and the repulsive force between the particles, causing osmotic consolidation [22]. In other words, salt interactions with clay modify soil microstructure by enlargement of macro porosity and shrinkage of microporosity due to higher attractive van der Waals forces. As a result, with the increase in salt concentration, the coarse diameter of macro-pores increases, and the density of soil micro-pores decreases. In this way, water-retention curves drop at low air entry value and steepen with increasing salt concentration afterward. To put it another way, there is more free water to drain and less retention capability at the same matric suction as molarity increases [10, 18].

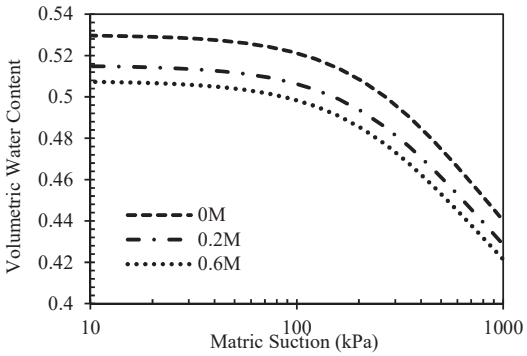

Fig. 2. Soil–water retention curves of clay core for various NaCl molar concentrations [20].

2.3 Hydraulic conductivity function

Hydraulic conductivity plays a crucial role in water flow analysis through saturated-unsaturated soils under steady-state or transient seepage. Additionally, previous studies showed that saline environments cause a significant microstructural evolution accompanied by an increase in macro porosity, which primarily governs flow characteristics and hydraulic conductivity [10]. Accordingly, in order to predict saturated hydraulic conductivity depending on salinity, a newly developed semi-empirical model is used [23]:

$$w_{Lc} = w_{L0} - \left(\frac{89.460}{1-\exp(2.595-0.007\times w_{L0})} - 7.152 \right) Ln(1+C) \quad (2)$$

$$k_{sat}(cm/s) = 6.992 \frac{\gamma_w}{\mu_w} \frac{1}{\rho_s^2} \frac{e^{0.625}}{1+e} \frac{1}{w_{Lc}^{2.039+0.947/e}} \quad (3)$$

$$\log(k_{sat}) = -10.220 \times \frac{w_{Lc}^{\left(\frac{0.031}{e}-\frac{2.778}{w_{Lc}}\right)}}{e^{\left(\frac{4.964}{w_{Lc}}-\frac{0.008}{e}\right)}} \quad (4)$$

where w_{Lc} is the liquid limit of soil if the solute concentration of pore fluid is equal to C, w_{L0} is the reference liquid limit for deionized water, k_{sat} is the saturated hydraulic conductivity (m/s), μ_w is the dynamic viscosity of water (Pa. s), γ_w is the unit weight of water (kN/m^3), ρ_s is the density of solid particles (kg/m^3), and e represents the void ratio. In this study, Eq. 3 and 4 were used for the clay core and earth fill parts of the dam, respectively. The values of saturated hydraulic conductivity for the earth fill and clay core parts of the dam under effect salt concentration materials are summarised in Table 1. The other parts of the dam materials are collected in Table 2. According to Table 1, saturated hydraulic conductivity increases with molar concentration. It could be due to the suppression of the diffuse double layer and increased macropores [23].

The unsaturated hydraulic conductivity is estimated in this study based on the Mualem-van Genuchten model considering SWRCs and saturated hydraulic conductivity with change in salt concentration. Hence, the unsaturated hydraulic conductivity model is modified based on the new saturated hydraulic conductivity models considering the effect of salt concentration. The adopted unsaturated relationship is defined as [17, 18, 23]:

$$k_w = k_s \frac{\left[1-(\alpha\psi^{(n-1)})\left(1+(\alpha\psi^n)^{-m}\right]^2\right.}{\left((1+\alpha\psi)^n\right)^{\frac{m}{2}}} \quad (5)$$

where kw is unsaturated hydraulic conductivity (m/s), ks is estimated based on the new model saturated conductivity (m/s).

The predicted unsaturated hydraulic conductivity of clay core materials is depicted in Fig. 3. According to this figure, as the molarity concentration increases, the permeability of soil is increased at the same matric suctions Some studies on saturated clay samples exposed to salt solution proved that the thickness of the diffuse double layer of clay decreases due to increased molar concentration. In other words, the effect of salt changes the microstructure of the soil because the van der Waals forces of attraction between clay particles increase, resulting in a decrease in soil micropores and an increase in macropores; therefore, the hydraulic conductivity increases [22, 24, 25].

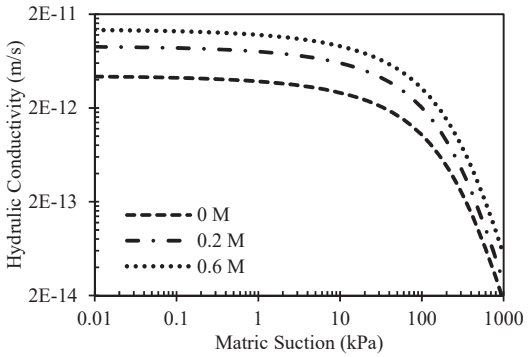

Fig. 3. Unsaturated hydraulic conductivity of clay core for various NaCl molar concentrations.

2.4 Rainfall Infiltration

The investigated site is located in the arid to semiarid regions of Iran. As a result, the amount of water infiltration is relatively low. According to the reported meteorological data of Rafsanjan station, the maximum amount of rainfall from January through March of the year 2017 is collected and reported in Fig. 4. As shown in this graph, the maximum rainfall intensity in the first, second, and third month is 3.4, 41, and 44 mm/day, respectively. These data have been used in numerical simulation to study the effect of rainfall infiltration on the dam slope instability [26].

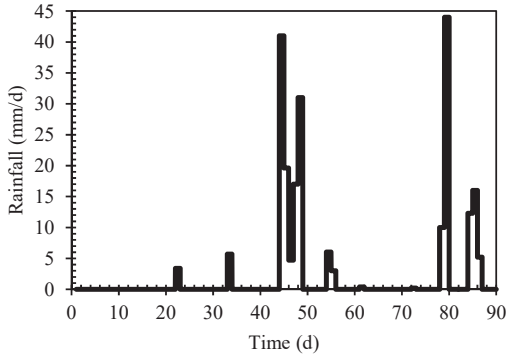

Fig. 4. Distribution of rainfall data for the Rafsanjan station during the period of Jan-Mar., 2017 [26].

3 Numerical Simulation

A two-dimensional analysis of the steady state and rainfall infiltration was conducted to investigate the effect of dissolved salts on saturated-unsaturated seepage and the stability of a tailings dam. Also, the concentrations of salts remain constant during the rainfall event. The GeoStudio software that is based on the finite element method has performed numerical analyses through SEEP/W and SLOPE/W modules for simulating precipitation and examining the factor of safety of the dam, respectively [27]. The geometry of the

numerical model is plotted in Fig. 1. Moreover, the mesh was created using quadrilateral and triangular elements. Based on mesh sensitivity analysis, the dimension of the quadrilateral elements was set at 1 m, and domain discretization was performed with 35883 nodes and 35443 elements [28, 29].

3.1 Seepage analysis

The Seep/W module was used to investigate rainfall infiltration because of its capabilities for simulating partially saturated flow in complex geometry with different materials. Two-step steady-state and transient seepage analyses were conducted to predict the location of the phreatic surface and to investigate the changes in pore water pressure regime in saline and distilled water conditions. The general governing differential equation of saturated-unsaturated seepage using Richard's equation can be written as [30]:

$$\frac{\partial}{\partial x}\left(k_x \frac{\partial H}{\partial x}\right)+\frac{\partial}{\partial y}\left(k_y \frac{\partial H}{\partial y}\right)+Q=\frac{\partial \theta}{\partial t} \quad (6)$$

where H is the total head, k_x is the hydraulic conductivity in the x-direction, k_y is the hydraulic conductivity in the y-direction, Q is the applied boundary flux, θ is the volumetric water content, and t is time. According to Eq. 6, hydraulic conductivity and water retention properties directly impact the seepage through an unsaturated medium under transient flow. Under steady-state conditions, on the other hand, the right-hand side term related to water retention characteristics vanishes, and hydraulic conductivity becomes the only factor governing the water flow.

3.2 Slope stability analysis

Following the seepage analysis, slope stability analyses are carried out in order to calculate the factor of safety against slope failure. Morgensen-Price's limit equilibrium method (LEM) is used to calculate the factor of safety. LEM is based on the method of slices, and the factor of safety is defined as the ratio between available and mobilized shear strength along the critical failure plane. In addition, the impact of the SWRCs salinity model is further highlighted by incorporating water retention properties and modified strength parameters as a function of salt molar concentration when estimating soil shear strength. Therefore, Vanapalli's modified Mohr-Coulomb equation is employed [31]:

$$\tau = c' + (\sigma_n - u_a)\tan\phi' + (u_a - u_w)\left(\frac{\theta_w - \theta_r}{\theta_s - \theta_r}\right)\tan\phi' \quad (7)$$

where τ is the shear strength at the failure, σ_n is the normal stress at the failure, u_a is air pressure, and u_w is water pressure. When dissolved salts in pore fluid diffuse to the clay surface, the effective stress formulation of Terzaghi should be extended to consider both the electrostatic repulsive pressure and the van der Waals force. This is due to the fact that previous studies revealed the significant role of osmotic suction on the mechanical properties of clayey soils. In other words, the influence of osmotic suction on saturated shear strength is significant on the high plasticity clay core. As a result, the variable governing the unsaturated shear strength of soil is both the soil-water retention curve and osmotic suction. Therefore, the saturated soil strength parameters corresponding to different compaction states are selected from Tables 3, and 4.

Table 3. Strength parameters for different dam sections.

Material	γ_t (kN/m^3)	c'(kPa)	ϕ'(°)
Earth fill	17	1	47
Clay core	21	7.53	110.5
Foundation	16	14	37.54
Filter	15	1	32
Rock fill	16	1	42
Tailings	18	26	7.5

Table 4. Variations in strength parameters of clay cores with NaCl molar concentrations [32].

Material	C (M)	c'(kPa)	ϕ'(°)
Clay core	0	110.5	7.53
	0.2	109.9	7.95
	0.6	106.04	9.43

4 Interpretation of the Results

4.1 Pore water pressure distributions

The pore water pressure distribution during rainfall infiltrations is shown in Fig. 5 for the cross-section specified by considering different salt concentrations at various time steps; Fig. 5 is based on the A-A cross-section of Fig. 1 depicted. The figure shows the distribution at initial, 30, and 60 days time steps. The hydroststic pressure considered as a initial hydraulic condition in this paper. According to this specific distribution, the pore water pressure dramatically increases during the first 30 days of the infiltration. With the increased rainfall in the last days, soil suction completely diminishes. Moreover, pore water pressure in all cases has changed up to 3 meters of the soil depth, and due to the low permeability of the materials, the amount of changes occurs at a small depth. As a result, the rain has little ability to pass through the dam.

The observed difference between the rate of infiltration in cases of salt concentrations and distilled water is due to the significant difference between the unsaturated hydraulic conductivities of the materials, based on Eq. 5 effect of salt on unsaturated hydraulic conductivity is considered. The differences between HCFs models due to the molar concentration are shown in Fig. 3. As a result, as soil salinity increases, infiltration ability intensifies due to increased unsaturated hydraulic conductivity, and the suction drop rate becomes more severe. As a result, water can

infiltrate the dam, and pore water pressure will increase significantly. Additionally, Fig. 6 shows the impact of salt concentration on increasing pore water pressure for the 30th day of rainfall at the 111m level for better understanding. The pore water pressure at the beginning equals -333 kPa for 0 molar concentration, which reaches -260 kPa with increased concentration.

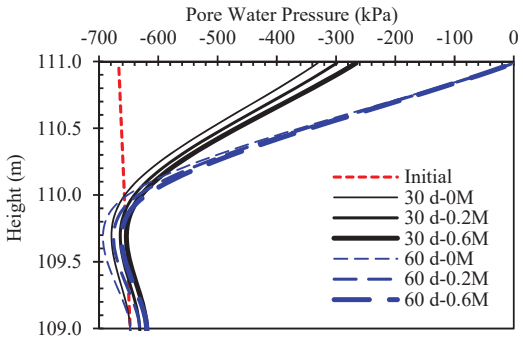

Fig. 5. Pore fluid pressure contours at different intervals from the rainfall for different molar concentrations.

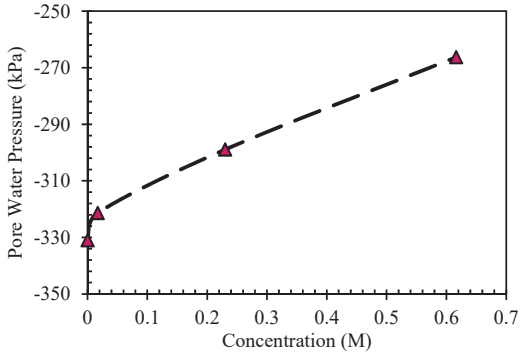

Fig. 6. Effect of NaCl molar concentrations on pore water pressure on the 30th day of rain at the level of 111m of height.

4.2 Factor of safety

Figure. 7 shows the effect of salt concentrations on the factor of safety under steady-state conditions. The results indicate that the safety factor improves slightly with increased salt concentration, and slope stability is somewhat enhanced compared to the initial state. The reason behind this is salt's effect on the shear strength parameters of dam clay core that is considered in this study. Previous research illustrated that in the high concentration, the diffuse double layer may be thinner, and the structure of the soil changes. Meanwhile, increasing salt concentration decreases the soil's porosity ratio, increases particle interaction, and increases shear strength. Additionally, the initial Pore water pressure distribution in the salinity and pure water models is the same; the other difference in these steady-state factors of safety is due to the unsaturated unit weights calculated according to the SWRCs. Increased molar concentration salinity models are drier than pure water models in the same suction. As a result, the unsaturated unit weight of salinity is less than that of pure water, and they have a higher factor of safety [8, 20, 29, 32].

Figure. 8 illustrates the variation of factors of safety for salinity and distilled water models during the rainfall incident. According to the results, all models' safety factors significantly decreased at the beginning stage, then at a meager rate, gradually increasing with decreased rainfall afterward. During the rainfall, due to the increase in saturation level, soil suction decreases; thus, soil shear strength decreases, leading to a sharp drop in the factor of safety. Moreover, on the days when there is no rain, due to the relatively higher permeability of the salt model compared to the water model [33], the water infiltrated through the dam body goes down at a higher rate, and the suction gradually increases, then shear strength is increased. As a result, the factor of safety is improved.

In general, During the precipitation event, the concentrations of salt constant affect flow characteristics and shear strength, including faster water drainage due to increased macropores and roughness and specific surface area of soil grains, which then increases interaction between soil particles, it caused salinity models to have a higher factor of safety [34, 35].

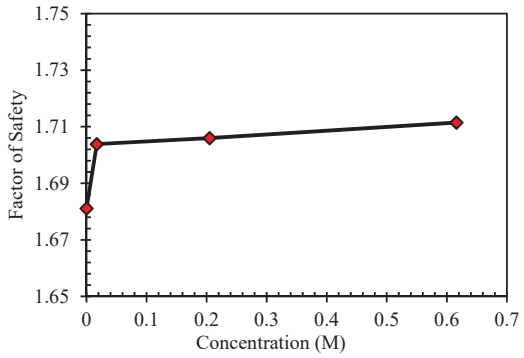

Fig. 7. Effect of NaCl molar concentrations on the factor of safety under steady-state conditions.

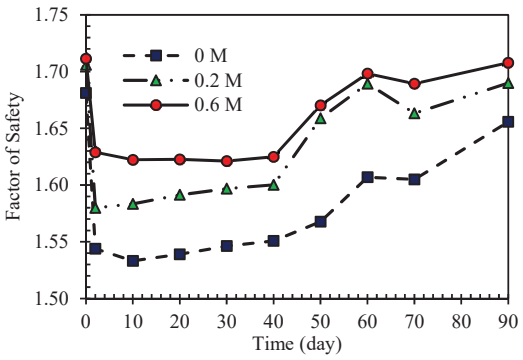

Fig. 8. Effects of NaCl molar concentrations on the factor of safety under transient conditions.

5 Conclusions

In this numerical study, the effects of NaCl molar concentrations on the pore water pressure regime and stability of a tailings dam were investigated under steady-state and transient conditions. In order to meet

this goal, models of soil-water retention and hydraulic conductivity dependent on salinity were used for modification of the unsaturated hydraulic conductivity model. The salinity model of soil-water retention illustrated that the retention capability of the soil decreases due to the increased osmotic consolidation in the matric suction. Additionally, the salinity-modified unsaturated hydraulic conductivity showed, according to the diffuse double layer theory, the swelling of clay diminished, and macroporosity was the enlargement. The results indicated that pore water salinity had a dramatic influence on the characteristics of seepage and stability analysis. According to the results of transient flow, the pore water pressure changes based on salt concentration showed that as molar concentration increased, the free water path became more, causing more rainfall to penetrate. As a result, the rate of suction reduction in these models was higher than in the pure water model. However, the factor of safety salinity models was higher than the pure water model due to unsaturated unit weights being calculated according to the SWRCs salinity, and the salinity effect was considered on shear strength parameters. Consequently, salt affects both flow and shear strength characteristics causing the seepage and stability analysis results to be changed compared to the simple state of pure water. Accordingly, the stability of the dam is improved by the simultaneous impact of salt on both the flow and strength. However, in this study, it was assumed that the concentrations of salts remain constant during the precipitation event. The study also does not include modeling the transport of salts.

Acknowledgments

The financial support provided by Iran National Science Foundation for “Experimental study of the hydro-mechanical behaviour of rooted soils in green stabilization of unsaturated slopes” by way of grant 4000730 is gratefully acknowledged. In addition, the authors are grateful to Iran's National Elites Foundation for supporting this research through the “Dr. Kazemi-Ashtiani Award.”

References

1. L. Piciullo, E.B. Storrøsten, Z. Liu, F. Nadim, S. Lacasse, Eng. Geol., **303**, 106-657 (2022)
2. S.G. Vick, BiTech Publ, Vancouver (1983)
3. A. Pak and M. Nabipour, Mine Water Environ., **36**, 341–355 (2017)
4. Z. Wei, G. Yin, J.G. Wang, L. Wan, G. Li, Waste Manag. Res., **31**, 106–112 (2013)
5. M.P. Davies, Geotech. News, 31–36 (2002)
6. R.S. Sharma and T.S. Al-Busaidi, Eng. Geol., **60**, 235–244 (2001)
7. B.G. Lottermoser and P.M. Ashley, J. Geochemical Explor., **85**, 119–137 (2005)
8. H. Sadeghi, A. Kolahdooz, M.M. Ahmadi, Yantu Lixue/Rock Soil Mech., **43**, 2136–2148 (2022)
9. H. Sadeghi, M. Kiani, M. Sadeghi, F. Jafarzadeh, Eng. Geol., **250**, 89–100 (2019)
10. H. Sadeghi and H. Nasiri, Geotech. Lett., **11**, 21–29 (2021)
11. H. Sadeghi and C.W.W. Ng, UNSAT (2018)
12. E. Ghazavi Baghini, Arab. J. Geosci., **9** (2016)
13. D. M. Franks, D. V. Boger, C. M. Côte, D. R. Mulligan, Resour. Policy, **36**,114–122 (2011)
14. M.M. Ahmadi, S.Kaheh, H. Sadeghi, A. Jamaat, Geo-Extreme, 311–317 (2021)
15. A.A. Garakani, M.M. Birgani, H. Sadeghi, Bull. Eng. Geol. Environ., **80**, 7525–7549 (2021)
16. A. Shamsai, A. Pak, S.M. Bateni, S.A.H. Ayatollahi, Geotech. Geol. Eng., **25**, 591–602 (2007)
17. M.T. Van Genuchten, Soil Sci. Soc. Am. J., **44**, 892–898 (1980)
18. H. Sadeghi and A. Golaghaei Darzi, MATEC Web Conf., **337**, 02001 (2021)
19. F. Zhang, C. Zhao, S.D.N. Lourenço, S. Dong, Y. Jiang, Bull. Eng. Geol. Environ., **80**, 717–729 (2021)
20. T. Thyagaraj and S.M. Rao, J. Geotech. Geoenvironmental Eng., **136**,1695–1702 (2010)
21. H. Yang, H. Rahardjo, E.C. Leong, and D.G. Fredlund, Can. Geotech. J., **41**, 908–920 (2004)
22. C. Di Maio, Géotechnique, **46**, 695–707 (1996)
23. A. Hedayati-Azar and H. Sadeghi, J. Contam. Hydrol., **249,** 104042 (2022)
24. T. Thyagaraj and M. Julina, Geotech. Lett., **9** ,348–354 (2019)
25. M. Zhang, H. Zhang, L. Jia, S. Cui, Nucl. Eng. Des., **250**, 35–41 (2012)
26. DEPATMENT MIran, Meteorological Organization (2022)
27. S. Sadat Naseri, , H. Sadeghi, , A. Akbari Garakani, Sharif J. Civ. Eng., **38**, 51–61 (2022)
28. GEO-SLOPE International Ltd., Geostudio Help, (2010)
29. GEO-SLOPE International, (2010)
30. U. Koyluoglu, Soil Dyn. Earthq. Eng., **12**, 449–450 (1993)
31. S.K. Vanapalli, D.G. Fredlund, D.E. Pufahl, A.W. Clifton, Can. Geotech. J., **33**, 379–392 (1996)
32. L. Zhang, D. Sun, D. Jia, Appl. Clay Sci., **132–133**, 24–32 (2016)
33. H. Sadeghi and P. AliPanahi, Eng. Geol., **278**, 105827 (2020)
34. H. Sadeghi, A.C.F. Chiu, C.W.W. Ng and F. Jafarzadeh, Sci. Iran., **27(2)**, 596–606 (2020)
35. C.W.W. Ng, H. Sadeghi, F. Jafarzadeh, M. Sadeghi, C. Zhou and S. Baghbanrezvan, Can. Geotech. J., **57(2)**, 221–235 (2020)